Transmission of 1—6-keV positrons through thin metal films

Allen P. Mills, Jr. and Robert J. Wilson
Bell Laboratories, Murray Hill, New Jersey 07974
(Received 4 November 1980)

We report measurements of the transmission of 1—6-keV energy positrons through films of Al, Cu, and Si up to 3000 Å thick. When the thickness is expressed in terms of mass per unit area, the transmission of Cu and Al is found to be the same within ±10%. Within a ±20% precision we observe no effect having to do with the crystallinity of the materials. The median penetration depth of positrons in Al and Cu is found to vary with the energy E as E^n, with $n=1.60^{+0.15}_{-0.08}$ and $1.43^{+0.07}_{-0.11}$, respectively. Our measured median penetration depths are significantly less than one would have expected from the calculation of Nieminen and Oliva [R. M. Nieminen and J. Oliva, Phys. Rev. B 22, 2226 (1980)] which seems to indicate the importance of large-angle scattering effects. Our measurements can be combined with independent measurements of the energy dependence of the yield of positronium at a surface [K. G. Lynn, Phys. Rev. Lett. 44, 1330 (1980) and K. G. Lynn and D. O. Welch, Phys. Rev. B 22, 99 (1980)] to obtain values for the positron diffusion constant D_+ in single-crystal metal samples. For example, we find $D_+(\text{Al})=(0.76\pm0.14)$ cm^2 sec^{-1} and $D_+(\text{Cu})=(1.06\pm0.20)$ cm^2 sec^{-1}. The former is in agreement with the deformation-potential calculation of Bergersen *et al.* [B. Bergersen, E. Pajanne, P. Kubica, M. J. Stott, and C. H. Hodges, Solid State Commun. 15, 1377 (1974)] if the positron effective mass in Al is $m_+=(1.59\pm0.12)m_e$. Finally, we use our measurements to calculate the optimum thickness of transmitting positron moderators for enhancing the brightness of slow positron beams.

I. INTRODUCTION

Low-energy positions which have been implanted into a solid target in vacuum form a unique and sensitive probe of the surface regions of the solid.[1,2] The positrons which diffuse to the surface may either become bound in the "image potential" well just outside the surface[3—10] or be ejected into the vacuum as free positrons[6] or positronium.[7,11] The relative likelihood of these three channels is sensitive to submonolayer surface contamination and the branching ratios may be found, for example, from measurements of the energy spectrum of the annihilation γ rays. On the other hand, the probability $L(E)$ of a positron reaching the surface after being implanted with energy E depends on the positron diffusion constant D_+ and annihilation rate γ_b in the bulk solid, the rate of trapping of positrons at crystalline defects γ_t, and the depth profile $p(x,E)$ of the positrons just after they stop in the solid.[7,12—16] Information about the parameters D_+, γ_b, and γ_t and their possible variation with depth x may be obtained from measurements of $L(E)$ if the depth profile is known.

In order to obtain information about how positrons stop in a metal, we have made measurements of the transmission probability for 1—6-keV energy positrons incident on thin films of Al, Cu, and Si. Before presenting the measurements, we must first ask if it is sensible to speak of positrons "stopping" in a metal. According to the calculations of Nieminen and Oliva[16] the rate of energy loss of a positron in Al is

$$dE/dt \approx 2\times10^{17}(E/1000\text{ eV})^{-1/2}\text{ eV sec}^{-1}$$

for $E>1000$ eV and reaches a maximum value of $dE/dt\approx3\times10^{17}$ eV sec^{-1} at $E\approx100$ eV. The total path length

$$\Delta s=\int_{E_{\min}}^{E_{\max}}\left[\frac{dE}{dt}\right]^{-1}(2E/m)^{1/2}dE \tag{1}$$

for positrons slowing down from an energy $E_{\max}$ to an energy $E_{\min}$ is roughly

$$\Delta s=500\text{ Å}(E_{\max}/1000\text{ eV})^2 \tag{2}$$

for $E_{\min}\approx100$ eV. While the positron is traveling along its path it will change its momentum as well as its energy, so Δs is an upper bound on how far the positron moves through the solid. At low energies $E<30$ eV, the energy loss rate is approximately

$$dE/dt \approx 2\times 10^{13}(E/1\text{ eV})^{5/2}\text{ eV sec}^{-1}$$

which for $E_{\max}\approx 100$ eV yields

$$\Delta s \approx 3\text{ Å}/(E_{\min}/1\text{ eV})\ . \tag{3}$$

By the time the positron has begun to undergo thermal diffusion ($E\approx 0.03$ eV), it is no more than ~ 100 Å from the position where its energy was ~ 100 eV and has spent a total time in the solid

$$\Delta t = \int_{E_{\min}}^{E_{\max}} \left[\frac{dE}{dt}\right]^{-1} dE \approx 2\times 10^{-12}(E_{\min}/0.03\text{ eV})^{-3/2}\text{ sec}\ . \tag{4}$$

We conclude that it makes sense to divide the history of a positron in a solid into two periods. At $t=0$ the positron passes through the vacuum-solid interface and starts to slow down. After a time short compared to the annihilation lifetime the positron has reached near-thermal energies and has a depth profile $p(x,E)$. During the second period ($t>\sim 2$ psec) the motion of the positrons may be calculated from the diffusion equation[17]

$$D_+\frac{\partial^2}{\partial x^2}\psi(x,t)=\frac{\partial}{\partial t}\psi(x,t)-(\gamma_b+\gamma_t)\psi(x,t)\ . \tag{5}$$

The initial condition on the positron density distribution $\psi(x,t)$ may be chosen to be

$$\psi(x,0)=p(x,E) \tag{6}$$

without introducing uncertainties greater than those associated with the ~ 100 Å smearing of $p(x,E)$ during the transition between the high-energy period ($E>100$ eV) and the thermal period ($E\approx 0.03$ eV).

II. EXPERIMENTAL

In our experiment we measure the probability $\eta(x,E)$ that a positron of energy E is transmitted by a film of thickness x, rather than $p(x,E)$. As we will show later, the depth profile $p(x,E)$ in a thick target is probably within a few percent of the approximate depth profile

$$p'(x,E)=-\frac{\partial}{\partial x}\eta(x,E) \tag{7}$$

which can be derived from our measurements.

It is important to keep in mind that our measurements are performed on samples that are either not free of defects or have a thick oxide layer at the surface. This means that once a positron has thermalized in the sample, it will not be reemitted as a slow positron[1] and we will not be confusing diffusion with transmission. On the other hand, our measurements of $\eta(x,E)$ are relevant to other work on clean single-crystal samples as shown later in Secs. IV B and V.

The apparatus for this experiment is shown schematically in Fig. 1. A positron beam of fixed energy E is limited by an aperture, passes through a metal film, and is guided by a ~ 150-G magnetic field down a 15-cm-diam drift tube to a distant 13-cm-diam Al foil annihilation target (biased at -100 V) and scintillation detector. Two Ni grids supporting Al and Cu graded-thickness films were bent into a semicircle with the metal layer outward and mounted in the vacuum chamber at the end of a manipulator shaft. A stepping motor turned the shaft in 0.0006 revolution increments every 0.9 sec so that various portions of the films moved in front of the 2.0-mm-diam aperture. Positrons coming through the aperture passed first through the Ni mesh, then through a thin C film substrate and finally into the metal film. The magnetic field was sufficient to ensure that all the transmitted positrons reached the target.

The graded-thickness films were prepared by evaporating the metal on ~ 100-Å-thick C substrates supported by 333-line-per-inch, 80% nominal transmission, ~ 4-μm-thick Buchbee Meers Ni mesh. The 99.999% pure Cu and Al were evaporated from W basked filaments located ~ 30 cm from the substrates and a quartz-crystal oscillator thickness gauge. An Archimedian spiral shutter just in front of the substrates was rotated at ~ 1 Hz during the evaporation to produce a linear density gradient 63.5 mm long. The deposition rates were ~ 15 Å sec^{-1} and ~ 5 Å sec^{-1} of Al and Cu, respectively. To ensure that the metal films were not lumpy on a scale greater than 100 Å, the Al (Ref. 18) was evaporated in 2×10^{-5} Torr O_2 and the Cu (Ref. 19) in 4×10^{-4} Torr Ar. High-background-pressure gases were used deliberately to suppress surface struc-

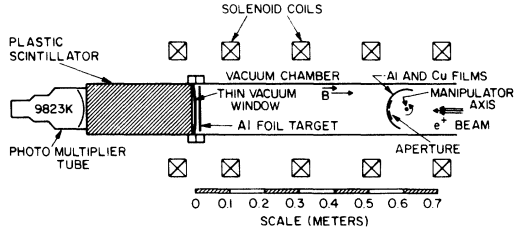

FIG. 1. Apparatus for measuring positron transmission through thin films.

ture,[19] currently important in Raman scattering, and tunneling experiments,[18] which may not have been considered in earlier transmission work. *In situ* evaporation onto liquid-He temperature substrates should eliminate such problems but poses extreme experimental difficulties. The absence of grains larger than 100 Å was confirmed by electron microscopy. Resistivity measurements would imply[18] that the Al grain sizes are probably <50 Å and that the O content could be as much as ~ 19 atomic % O at a thickness $x=2400$ Å, $\sim 25\%$ at $x=1000$ Å, and $\sim 50\%$ at $x=300$ Å, but discontinuities in the film may also increase the resistivity. While Al_2O_3 tends to increase the film density, the graininess of the film tends to reduce it. These effects nearly canceled because the density of Al coevaporated with the sample was 2.65 ± 0.4 g/cm^3, essentially the same as bulk Al.

The grain size of the samples is an important consideration. If the mean film thickness becomes less than the grain size, the measured $\eta(x,E)$ may not reflect the true distribution one would find in a thick sample. The possible influence of the presence of impurities and the polycrystalline nature of the films will be addressed later on when we compare the graded-thickness film results with measurements on polycrystalline films evaporated in ultrahigh vacuum *(in situ)* and on single-crystal films.

The film thickness on glass substrates next to the C substrates was measured using a Dektac thickness gauge. The measured thickness gradients (see Fig. 2) are (41.7 ± 0.9) Å/mm and (18.4 ± 0.5) Å/mm for the Al and Cu films, respectively. The film thickness was also measured by weighing portions of the films which had been floated off onto glass slides of known weight. We obtain mass densities of (72 ± 10) μg/cm^2 for Al and (110 ± 5) μg/cm^2 for Cu averaged over a 10-mm-long part of the films at the thickest end. These results agree with the thickness gauge measurements of Fig. 2.

The positron beam position could be moved by a pair of deflection coils. Before each run, the position was adjusted to maximize the number of positrons passing through the aperture with the sample films removed. The relative number of positrons of incident energy E passing through the films versus position along the film was measured by recording the total annihilation photon count rate $V(s,E)$ versus stepper motor step number s using a 1024-channel multiscaler. An example of two measurements of $V(s,E)$ obtained with $E=4175$ and 24 eV is shown in Fig. 3. The positions of the two graded-thickness films are indicated. An opaque post and a gap in the Ni mesh provided count rates for background subtraction and normalization, respectively. The count rate change when a support wire passed in front of the aperture (at steps 380 and 835) shows the position resolution is about five steps corresponding to $\sim 1.6\%$ of the maximum film thickness. The pattern starts to repeat beyond step 840 but the 2 films are overlapping (the manipulator axis was displaced slightly from the beam axis).

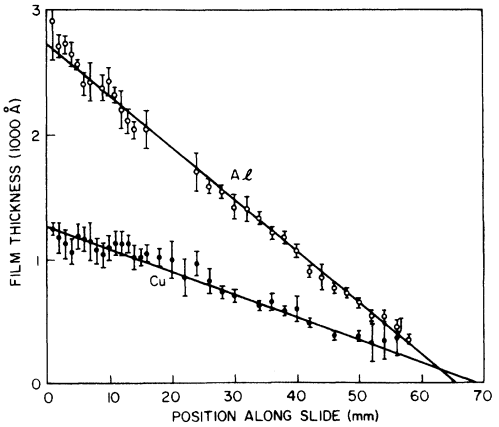

FIG. 2. Measured film thickness vs position for the graded-thickness Al and Cu films.

III. RESULTS

The transmission coefficient of positrons through the metal films $\eta(s,E)$ is computed from the background subtracted, normalized count rates $V(s,E)$ after correcting for the grid transmission coefficient A and the presence of holes in the sample films. We presume that the grids absorb a constant fraction of the incident positrons at all incident energies. Holes, which appear during the flotation of the carbon support from its mica substrate prior to metalization, are assumed to be perfectly transmitting. The effective area of a hole can be obtained from the very-low-energy count rate $V(s,E\approx 0)$ with $E=24$ eV. We then have

$$\eta(s,E)=[V(s,E)-V(s,0)]/[A-V(s,0)] . \quad (8)$$

A was measured at a portion of the grids which was not covered by the C or metal films. We obtained $A=0.659\pm 0.004$ independent of the sample position s.

The transmission versus thickness x, $\eta(x,E)$, calculated from Eq. (8) is presented in Figs. 4 and 5 for Al and Cu films and $E=1-6$ keV. The thick-

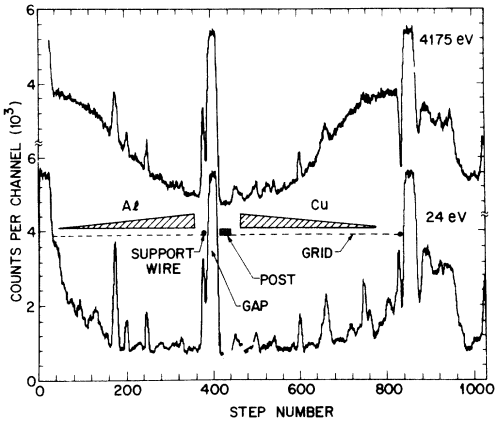

FIG. 3. Transmitted positron counts per 0.9-sec step for 24- and 4175-eV positrons.

ness x is obtained from the sample position s using Fig. 2 and the known geometry of the samples. The thickness gradients were not sharply cut off at the thin end of the films and the point of zero metal thickness is uncertain. Because of this and also because of the C support film thickness there is no data for $x<180$ Å Al or for $x<50$ Å Cu. For the Al curves with $180<x<320$ Å and the Cu films with $50<x<90$ Å the thickness scale has been obtained from the $E=4.1$-keV transmission coefficient η assuming $\eta(x,4.1\text{ keV})$ is linear for $x<320$ Å Al or 90 Å Cu, respectively. The fitted curves are ratios of two quadratics,

$$\eta(x)=(1-x/x_0)^2(1-\alpha x/x_0 + \beta x^2/x_0^2)^{-1}\theta(1-x/x_0)\,. \quad (9)$$

It is interesting to note that the nonzero slope of

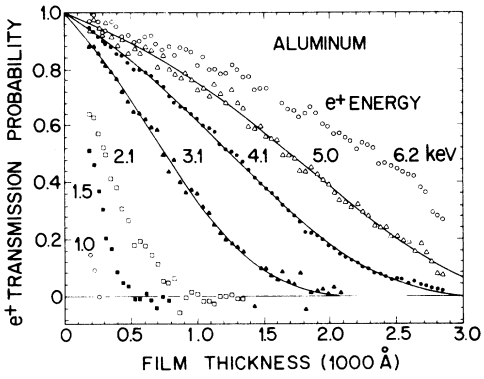

FIG. 4. Positron transmission probability vs film thickness and positron energy for Al evaporated on a Ni-mesh-supported ~100-Å-thick C film. The uncertainties due to counting statistics are small compared with the hole-correction errors [see Eq. (8)]. The fitted curves have the form of Eq. (9) with parameters listed in Table I.

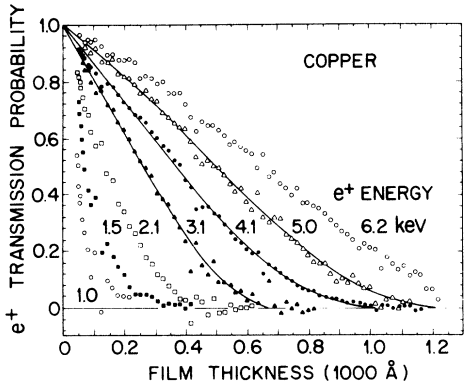

FIG. 5. Positron transmission probability vs film thickness and positron energy for Cu films (see caption to Fig. 4).

$\eta(x,E)$ near $x=0$ is an indication of the importance of large-angle scattering and of highly inelastic interband transitions. Except for the linear dependence on x near $x=0$ and the quadratic approach to zero transmission at $x=x_0$, the curves have no theoretical basis. The best-fit parameters for three curves each of Cu and Al are listed in Table I.

IV. DISCUSSION

A. Backscatter effect

Shown in Fig. 6 are the depth profiles $p'(x)$ for Al, taken to be the negative derivative of the fitted curves. We will now consider the magnitude of the difference between $p'(x)$ and the true depth profile $p(x)$ that would be measured in a thick target. If such a target is thought of as being divided in two by a plane located at a depth x, then some of the implanted positrons may cross this plane more than

TABLE I. Parameters for Eq. (9) which fit the Al and Cu data in Figs. 4 and 5. x_0 is the maximum range; initial slope is $\eta'(0)=(-2+\alpha)/x_0$.

Film	e^+ Energy (keV)	x_0 (Å)	α	β
Al	3.1	2150	0.93	1.31
	4.1	3125	1.11	1.03
	5.0	3650	1.31	0.82
Cu	3.1	691	0.70	0.34
	4.1	1035	0.60	0.50
	5.0	1246	0.97	0.70

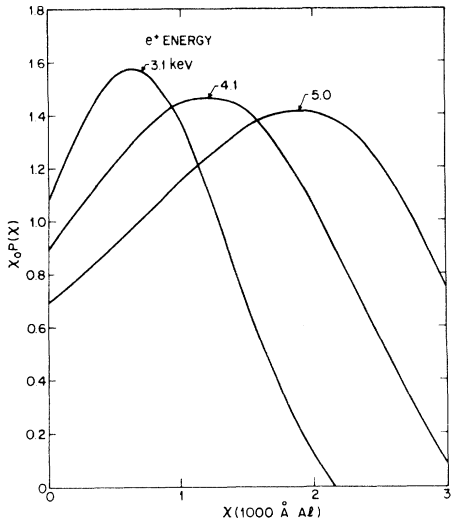

FIG. 6. Stopping profiles for positrons in Al found by taking the negative of the first derivative of the curves in Fig. 4.

once. In the geometry of Fig. 1 this effect is present to first order since positrons transmitted through the sample film may be backscattered from the Al foil annihilation target. Second-order scattering effects are not represented correctly by our geometry because the sample film is small compared to the lateral spread of the transmitted positron beam.

To obtain an estimate of the error caused by these scattering effects we have measured the integral longitudinal energy spectrum of 0.5-, 1.0-, 2.0-, and 2.9-keV positrons backscattered from an Al foil target (see Fig. 7). We see that over 90% of the secondary positrons have a longitudinal energy component less than half the energy of the primary positron. The total backscatter probabilities $P(E)$ for 0.5-, 1-, 2-, and 2.9-keV positrons are estimated ($\pm 10\%$) from Fig. 7 to be 0.040, 0.060, 0.084, and 0.10, respectively. These measurements fall on a curve $P(E)=0.06(E/1\text{ keV})^{1/2}$. Extrapolating to $E=6$ keV we conclude that the backscatter probability is less than 15% for $E<6$ keV and that the second-order backscatter effect should make less than a 1.5% error in our measurements. We assume the error is also negligible for the Cu measurements.

B. Sample preparation effects

The graded-thickness films used in the above measurements are not single crystals, are contaminated with impurities, and are supported by a Ni mesh and C film. Before we can conclude that these measurements tell us about positron depth

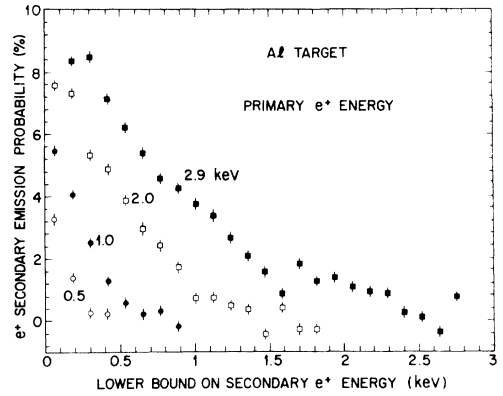

FIG. 7. Positron secondary-emission probability vs the lower bound on the normal component of the secondary positron energy for 0.5—2.9-keV positrons incident on an Al foil target.

profiles in the clean single-crystal samples currently being studied by the slow positron techniques,[2] we must examine the effect of each of these perturbations.

In Figs. 8 and 9 we present measurements of the positron transmission probability for Al and Cu films deposited *in situ* in ultrahigh vacuum ($<10^{-7}$ Torr during evaporation, $<10^{-9}$ Torr following evaporation). In each case the annihilation target was made of the same metal as the film. The C substrates for the Al and Cu films were both taken from the same C-coated mica sheet and therefore have the same thickness x_c. We define the median penetration depth $x_{1/2}$ for positrons of energy E by $\eta(x_{1/2},E)=\frac{1}{2}$. Tables II and III and Fig. 10 contain $(x_{1/2},E)$ values read off Figs. 4, 5, 8, and 9. For the graded-thickness films the $x_{1/2}$ values in

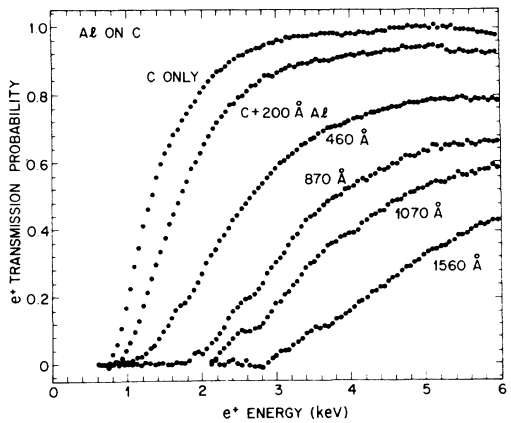

FIG. 8. Positron transmission probability vs energy for Al evaporated on a carbon film *in situ*. The C thickness is estimated from Fig. 10 to be $(5\pm1)\times10^{-6}$ g/cm^2, equivalent to 190 Å of Al.

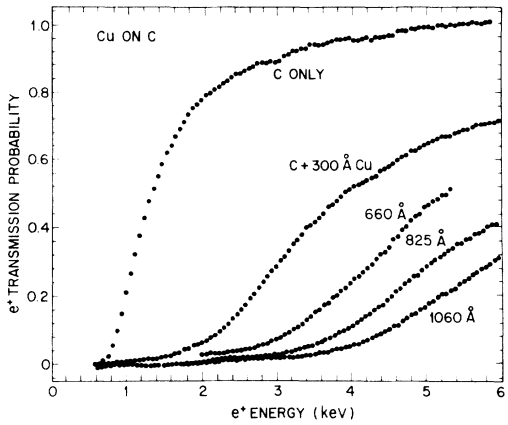

FIG. 9. Positron transmission probability vs energy for Cu evaporated on a carbon film *in situ*. The C film was the same thickness as the one in Fig. 8.

Table II include a contribution from the ~100-Å-thick C substrate. Within the experimental accuracy, $x_{1/2}$ expressed in terms of mass per unit area is the same for the graded-thickness Cu and Al films and can be fitted by a power law $x_{1/2}(E)=aE^n$ with $n=1.60^{+0.15}_{-0.08}$ for Al and $n=1.43^{+0.07}_{-0.11}$ for Cu. Lynn and Lutz[20] have found $n=1.6\pm0.1$ from a study of the positronium yield of thick targets versus incident positron energy. The solid line in Fig. 10 is the best fit to the graded-thickness Al data; with E in keV, the proportionality constant is $a=(3.32^{+0.84}_{-0.70})\times10^{-6}$ g/cm^2.

The C substrate for the *in situ* deposited films transmitted one-half the positrons when their energy was 1300±50 eV (see Figs. 8 and 9). Assuming the lack of Z dependence exhibited by the graded-thickness Al and Cu data in Fig. 10 can be extended to C too, we estimate from the solid curve in Fig. 10 that the *in situ* C substrate thickness is

TABLE II. Median penetration depth $x_{1/2}$ for various energy positrons in Al and Cu based on graded-thickness film measurements including the ones shown in Figs. 4 and 5.

e^+ Energy (eV)	$x_{1/2}$ (10^{-7} g/cm^2) Al	Cu
1000	26(16)	41(16)
1500	51(16)	57(16)
2075	80(16)	120(18)
2481	133(18)	161(19)
3110	201(19)	234(21)
3500	261(20)	268(22)
4130	342(22)	331(23)
4469	386(23)	367(25)
4885	444(25)	422(26)
4999	458(25)	444(26)
6153	627(28)	580(30)

TABLE III. Positron energy $E_{1/2}$ for 50% transmission through Cu, Al, and Si films (see Figs. 8, 9, and 11).

Sample	Film thickness (10^{-7} g/cm^2±10%)	$E_{1/2}$ (eV±10%)
Cu + C	320	3900
	640	5300
Al + C	105	1700
	175	2700
	285	3800
	340	4800
Si(110)	530	4480

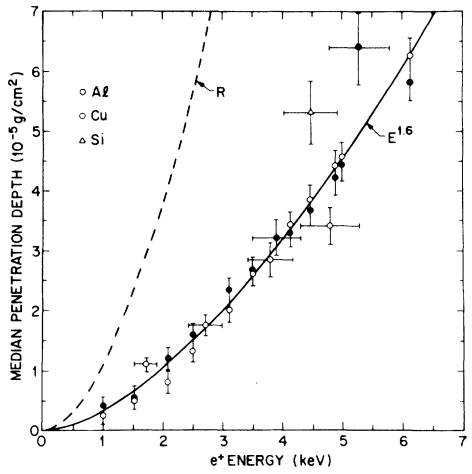

FIG. 10. Median penetration depth of positrons in thin films of Al, Cu, and Si. Single error bar points were obtained by finding the thicknesses $x_{1/2}$ corresponding to 50% transmission for a fixed positron energy. Points which have an error bar corresponding to an energy uncertainty as well as a thickness uncertainty were obtained by estimating the energy $E_{1/2}$ for half transmission through a foil of given thickness. Curve R is the mean penetration depth for positrons in Al as calculated by Nieminen and Oliva, Ref. 16. Solid curve is a fit of the function $x_{1/2}(E)=aE^n$ to the graded-thickness Al data with the single error bars. With E in keV, the best fit gives $a=(3.32^{+0.84}_{-0.70})\times10^{-6}$ g/cm^2 and $n=1.60^{+0.15}_{-0.08}$. Error estimates stem principally from a possible systematic uncertainty $(^{+2.7}_{-1.4})\times10^{-6}$ g/cm^2 in the thickness. Data for this figure are given in Tables II and III.

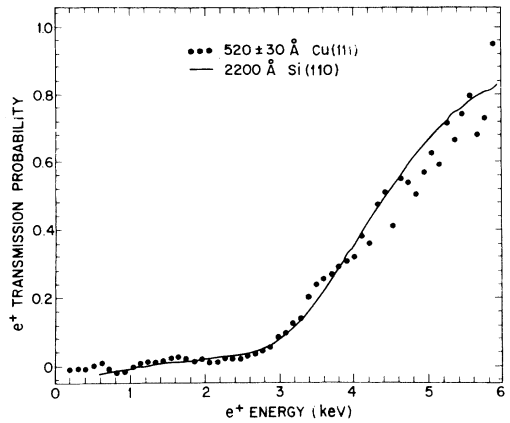

FIG. 11. Positron transmission probability vs energy for a self-supporting Si(110) crystal and a mesh-supported Cu film grown on mica. There is uncertainty of as much as $^{+0}_{-20}\%$ in the scale height because the energy was not high enough to ensure 100% transmission. Spread in the Cu data is due to variations in the positron beam strength as the source energy was ramped. Si data are represented by a line connecting the 10^3 points.

$x_c = (5 \pm 1)\ \mu g\,cm^{-2}$. This thickness has been added to the metal thicknesses in Table III. The pairs of $(x_{1/2}, E_{1/2})$ values thus obtained (double error flags in Fig. 10) agree with the graded-thickness film data in Fig. 10. We conclude that depositing the metal films *in situ* does not change the positron stopping profile significantly (less than $\sim 10\%$ effect).

There remains the possibility that there is a significant effect due to the C film, the Ni mesh, and the polycrystallinity of the films. Figure 11 shows the positron transmission probability versus positron incident energy for a free standing single-crystal Si(110) film[21] and a mesh-supported Cu film. The former was fabricated by ion-implant doping and subsequent etching; the latter was formed by evaporating Cu onto a mica substrate[22] in ultrahigh vacuum, floated off onto a water surface, and picked up on a Ni mesh. The probability scale is only approximate since very-high-energy positrons were not available to determine the count rate corresponding to 100% transmission. Within the error estimate including the latter uncertainty the energies corresponding to 50% transmission are in agreement with the other measurements in Fig. 10 (see also Table III). There may be as much as a 20% greater mean penetration depth in the Si(110), an effect which might be expected because of positron channeling.[23] However, since the estimated error in the Si thickness is $\pm 10\%$, this is not conclusive. We conclude that the effects associated with the C substrate, the Ni grids, and the sample crystallinity are negligible at the present level of accuracy.

C. Comparison with theory

The line labeled R in Fig. 10 is taken from Nieminen and Oliva's calculation[16] of positron mean stopping depths for Al. The energy dependence of this curve is $E^{1.8}$; none of the measurements are consistent with this calculation. The most likely explanation for this discrepancy is that the calculation has essentially assumed the large-angle scattering cross section is a Gaussian function of the scattering angle. This approximation completely neglects the occasional very-large-angle Rutherford scattering from the ion cores of the solid. In fact, the curve R is in better agreement with the present measurements if it is compared to the maximum path length $\Delta s(E)$. In Fig. 12 we see that the Nieminen and Oliva curve R is close to the values of $\Delta s(E)$ obtained from Figs. 3, 4, 8, 9, and 11 by estimating the thickness or energy at which positron transmission just begins (the data so obtained is also given in Table IV). Further indications that large-angle scattering plays a significant part in shortening the mean penetration depth are that the derived depth profiles in Fig. 6 do not vanish for zero depth and are not sharply peaked, contrary to the predictions of Ref. 16.

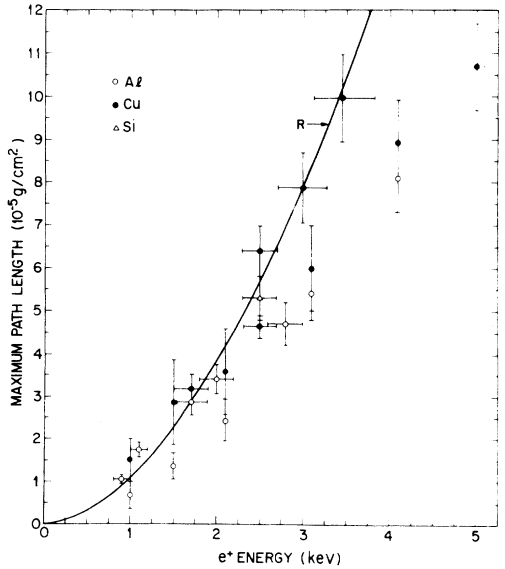

FIG. 12. Estimated maximum path length vs positron energy. The data are given in Table IV. Curve R is the same as in Fig. 10.

TABLE IV. Energy E_{min} at which positrons start to be transmitted through thin films.

Sample	Film thickness (10^{-7} cm^2/g)	E_{min} (eV)
Si(110)	530(53)	2500(200)
Cu(111)	464(47)	2500(200)
Cu + C	318(32)	1700(170)
	639(64)	2500(250)
	787(79)	3000(300)
	1000(100)	3400(340)
Al + C	104(10)	900(100)
	174(17)	1100(100)
	285(29)	1700(200)
	339(34)	2000(200)
	471(47)	2800(200)
Al wedge + C	68(30)	1000
	135(30)	1500
	243(50)	2075
	540(60)	3110
	810(80)	4130
Cu wedge + C	150(50)	1000
	286(100)	1500
	357(100)	2075
	598(100)	3110
	893(100)	4130
	1070(100)	5000

D. Comparison with e^- measurements

Several experimenters have reported measurements of the transmission of electrons through thin films[24–26] at energies below 10 keV. As expected, the transmission probabilities $\eta_+(x,E)$ and $\eta_-(x,E)$ have similar shapes. Table V lists, for various film thicknesses, the electron energy for 50% transmission $E_{1/2}$ estimated from the data of Refs. 24–26. The last column of the table is the median penetration depth $x_{1/2}$ for positrons of energy $E_{1/2}$ based on the solid curve in Fig. 10. Eight of the 12 entries in the table show agreement between the electron and positron values of $x_{1/2}$ to $\sim\pm10\%$. The remaining four entries show an $x_{1/2}$ for electrons which is significantly larger than for positrons. However, these data are contradicted by the other electron data and we cannot conclude that electrons penetrate farther than positrons.

V. APPLICATIONS

A. Diffusion constants

We turn now to a brief discussion of one application of our results—the measurement of positron diffusion constants. It is well known[12–16] that the probability that a positron of initial energy E is lost from the surface after being implanted into a solid

TABLE V. Electron transmission data from the literature, Refs. 24–26. The $E_{1/2}$ column gives the electron energy for 50% transmission; the $x_{1/2}$ column gives for comparison the thickness that would transmit 50% of positrons of energy $E_{1/2}$.

Film	Thickness (μg/cm^2)	$E_{1/2}$[d] (keV)	$x_{1/2}$[e] (μg/cm^2)
Aluminized	24±3[a]	3.5	26
collodion	32±3[a]	4.0	32
collodion	39±3[a]	4.5	39
collodion	68±3[a]	6.5	70
Cu	85±10[b]	7.1	81
Si	40±5[b]	3.7	28
Si	80±10[b]	7.2	82
Ge	60±7[b]	4.6	40
Ge	93±10[b]	6.8	75
Al_2O_3	5[c]	1.1	4
Al_2O_3	44[c]	4.5	39
Al_2O_3	94[c]	7.1	81

[a]Lane and Zaffarano, Ref. 25.
[b]Viatskin and Makhov, Ref. 24.
[c]J. R. Young, Ref. 26.
[d]Energy for 50% transmission, read off graphs in the above references.
[e]Thickness for 50% transmission of particles with energy $E_{1/2}$ based on curve in Fig. 10, $x_{1/2}=70\ \mu g/cm^2\ (E/6.55\ keV)^{1.6}$.

target is proportional to the Laplace transform of the stopping profile,

$$L(\xi,E)=\int_0^\infty p(x,E)e^{-\xi x}dx$$
$$=1-\xi\int_0^\infty \eta(x,E)e^{-\xi x}dx\ . \qquad (10)$$

The variable ξ is the inverse diffusion length $\xi=\sqrt{\gamma/D_+}$ in the simplest case, where γ is the bulk annihilation rate and D_+ is the positron diffusion constant. Figure 13 shows our data transformed according to Eq. (10). To find the positron diffusion length in Al we look at Lynn's data[27] to find that at $E=4030$ eV only 36% of the positrons at 300 K reach the surface (see Fig 1, Ref. 27). Now we read $\xi^{-1}=(3.03\pm0.23)\times10^{-5}$ g/cm^2 from the appropriate curve in our Fig. 13 and using a recent value[28] for the positron annihilation lifetime in bulk Al ($\tau=166$ psec) we find $D_+=(0.76\pm0.14)$ cm^{2}sec^{-1}, where the error estimate is $\pm16\%$ statistical and $\pm10\%$ systematic added in quadrature. In a similar way we find[13] that in Cu 72(2)% of the positrons reach the surface having been implanted at 4.1 keV. Using $\tau=118(2)$ psec[29] we find $D_+=(1.06\pm0.20)$ cm^{2}sec^{-1} for Cu.

These new and relatively precise values for the positron diffusion constant are in agreement with most estimates from other experiments.[5,30–43] For example, from room-temperature extrapolations of positron mobility measurements in Ge (Ref. 34) and Si (Ref. 43) we have at 300 K $D_+(\text{Ge})\approx0.55$ and $D_+(\text{Si})\approx1.56$ cm^{2}sec^{-1}.

The theoretical expression for the positron diffusion constant D_+ is obtained from the Nernst-Einstein relation $D_+=\mu_+kT/e$ and the mobility calculation of Bardeen and Shockley[44] which takes into account the interaction of a mobile charge carrier with longitudinal acoustic phonons:

$$D_+=(8\pi/9)^{1/2}\hbar^4\langle c_{ii}\rangle m_+^{-5/2}\epsilon_d^{-2}(kT)^{-1/2}\ . \qquad (11)$$

Here $\langle c_{ii}\rangle$ is the elastic constant[45] associated with longitudinal waves averaged over the direction of propagation, m_+ is the positron effective mass, and ϵ_d is the deformation potential. This is identical to the expression of Nieminen and Oliva[16] and Bergersen *et al.*[46] except that their numerical factor is $(\pi^2/3)^{1/2}$ which makes the expression 1.085 times larger than Eq. (11). Using[44,45] $\langle c_{ii}\rangle\approx\frac{1}{2}(c_{11}+c_{12}+2c_{44})=1.120\times10^{12}$ dyn cm^{-2}, $T=300$ K, and the Bergersen *et al.* calculation[46] $\epsilon_d=0.63$ Ry we have for Al

$$D_+=2.41(m_+/m_e)^{-5/2}\ \text{cm}^2\text{sec}^{-1}\ . \qquad (12)$$

The Bardeen and Shockley expression, Eq. (11), contains two quantities which are not very precisely known: the positron effective mass m_+ and the deformation potential ϵ_d. Our measurement of D_+ for Al is in agreement with Eq. (12) if $m_+=(1.59\pm0.12)m_e$, a value that is not far from the phenomenological value $1.8m_e$ chosen by Bergersen *et al.*[46]

B. Brightness enhancement

The basic limitation on how tightly one can focus a particle beam is set by Liouville's theorem which implies that the brightness per unit energy R of a beam of S particles per second,

$$R=S(\sin^2\theta d^2E)^{-1}\ , \qquad (13)$$

is a conserved quantity. In this expression E is the beam energy, d its diameter, and θ its angular divergence. However, when positrons slow down in a moderator crystal, R actually increases several orders of magnitude due to the presence of nonconservative forces. We can make further gains in the brightness of a positron beam by repeated stages of

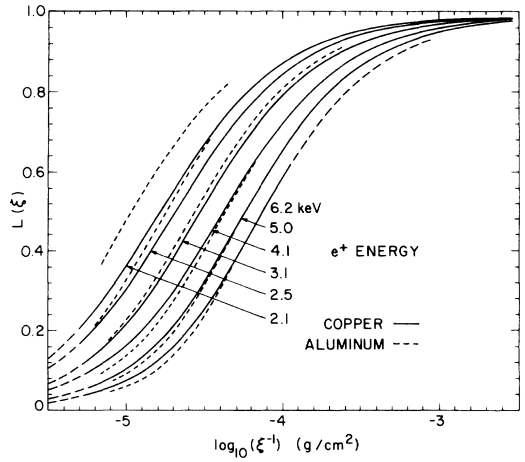

FIG. 13. Laplace transform of the data in Figs. 4 and 5.

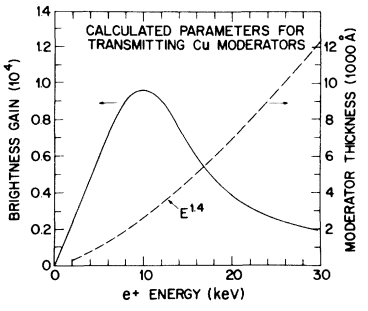

FIG. 14. Calculated parameters for transmitting Cu moderators.

moderation, acceleration, and focusing.[47] One way of achieving this would be to use thin single-crystal secondary moderators which would emit slow positrons from the front while being irradiated on the back with high-energy focused positrons.

Now that we know how positrons stop in a solid we can predict the properties of these secondary moderators. As a first approximation we assume that positrons of energy E stop uniformly and completely in a Cu moderator[48,49] whose thickness is proportional to $E^{1.4}$ (see dashed curve in Fig. 14). For such a uniform stopping profile it is easy to show that the number of positrons reaching one surface of a moderator film of thickness d is

$$L=(4/\pi^2)\sum_{n=0}^{\infty}[(2n+1)^2+d^2/\pi^2 D_+\tau]^{-1}\,, \qquad (14)$$

where $\sqrt{D_+\tau}$ is the positron diffusion length. The brightness gain for such a moderator (solid curve in Fig. 14) is roughly the quantity L times the slow positron reemission probability which is about 60% for a Cu(111) + S surface. From Fig. 14 we see that the best brightness gain, 10^4, would occur for a primary positron energy of 10 keV and a transmitting Cu moderator thickness of 2600 Å. As discussed in Ref. 47, brightness enhanced positron beams would be very useful for imaging crystalline defects using a positron microprobe, for surface studies using positron diffraction, for differential positron-atom scattering cross section measurements, and for many new experiments which would be possible with a very intense positron flux.

ACKNOWLEDGEMENTS

It is a pleasure to acknowledge helpful discussions with W. Brandt, A. Hebbard, K. G. Lynn, C. A. Murray, R. M. Nieminen, P. M. Platzman, and J. E. Rowe.

[1]W. Brandt, in *Radiation Effects on Solid Surfaces, Advances in Chemistry Series,* edited by M. Kaminsky (American Chemical Society, Washington, D.C., 1976), Vol. 158, p. 219.

[2]For recent reviews see the lecture notes by A. Mills and K. Lynn, in *International School of Physics,* "Enrico Fermi", 1981, edited by W. Brandt and A. Dupasquier (in press).

[3]C. H. Hodges and M. J. Stott, Solid State Commun. 12, 1153 (1973).

[4]R. M. Nieminen and M. Manninen, Solid State Commun. 15, 403 (1974).

[5]A. Gainotti and C. Ghezzi, Phys. Rev. Lett. 24, 349 (1970).

[6]A. P. Mills, Jr., P. M. Platzman, and B. L. Brown, Phys. Rev. Lett. 41, 1076 (1978).

[7]A. P. Mills, Jr., Phys. Rev. Lett. 41, 1828 (1978).

[8]K. G. Lynn, Phys. Rev. Lett. 43, 391 (1979); 43, 803 (1979).

[9]A. P. Mills, Jr., Solid State Commun. 31, 623 (1979).

[10]I. J. Rosenberg, A. H. Weiss, and K. F. Canter, J. Vac. Sci. Technol. 17, 253 (1980).

[11]K. F. Canter, A. P. Mills, Jr., and S. Berko, Phys. Rev. Lett. 33, 7 (1974).

[12]W. Brandt, Appl. Phys. 5, 1 (1974).

[13]K. G. Lynn and D. O. Welch, Phys. Rev. B 22, 99 (1980).

[14]A. P. Mills, Jr. and C. A. Murray, Appl. Phys. 21, 323 (1980).

[15]J. Oliva, Phys. Rev. B 21, 4909 (1980); 21, 4918 (1980); 21, 4925 (1980).

[16]R. M. Nieminen and J. Oliva, Phys. Rev. B 22, 2226 (1980).

[17]The energy dependence of D_+ and γ_t may be important, thus necessitating the solution of the Boltzmann equation rather than Eq. (5) as pointed out by W. Brandt and N. R. Arista, Phys. Rev. A 19, 2317 (1979).

[18]G. Deutscher, H. Fenichel, M. Gershenson, E. Grunbaum, and Z. Ovadyahu, J. Low Temp. Phys. 10, 231 (1973); P. Ziemann, G. Heim, and W. Buckel, Solid State Commun. 27, 1131 (1978).

[19]C. A. Murray and J. E. Rowe (private communications). See J. V. Sanders, in *Chemisorption and Reactions on Metal Films,* edited by J. R. Anderson, (Academic, New York, 1971), p. 1.

[20]K. G. Lynn and H. Lutz, Phys. Rev. B 22, 4143 (1980).

[21]We thank L. Feldman for giving us this sample.

[22]This technique presumably results in an epitaxial Cu(111) film; see R. L. Palmer, J. N. Smith, H. Saltsburg, and D. R. O'Keefe, J. Chem. Phys. 53, 1666 (1970).

[23]J. V. Andersen, W. M. Augustyniak, and E. Uggerhøj, Phys. Rev. B 3, 705 (1971).

[24]A. I. Viatskin and A. F. Makhov, Zh. Tekh. Fiz. 28, 740 (1958) [Sov. Phys.—Tech. Phys. 3, 690 (1958)]; A. F. Makhov, Fiz. Tverd. Tela (Leningrad) 2, 2161 (1960); 2, 2172 (1960); 2, 2176 (1960) [Sov. Phys.—Solid State 2, 1934 (1960); 2, 1942 (1960); 2, 1945 (1960)]; H. J. Fitting, Phys. Status Solidi A 26, 525 (1974); H. J. Fitting, J. Phys. D 8, 1480 (1975).

[25]R. O. Lane and D. J. Zaffarano, Phys. Rev. 94, 960 (1954).

[26]J. R. Young, Phys. Rev. 103, 292 (1956).

[27]K. G. Lynn, Phys. Rev. Lett. 44, 1330 (1980).

[28]M. J. Fluss, L. C. Smedskjaer, M. K. Chason, D. G. Legnini, and R. W. Siegel, Phys. Rev. B 17, 3444

(1978).
[29]L. C. Smedskjaer, M. J. Fluss, D. G. Legnini, M. K. Chason, and R. W. Siegel, J. Phys. F 7, 1715 (1977).
[30]For a review see R. Paulin, in *Positron Annihilation,* proceedings of the 5th International Conference, Japan, 1978, edited by R. Hasiguti and K. Fujiwara (Japanese Institute of Metals, Aboba Aramaki, Sendai 980, Japan, 1979), p. 601.
[31]G. Lang and S. DeBenedetti, Phys. Rev. 108, 914 (1975).
[32]I. K. MacKenzie and J. L. Campbell, Nucl. Instrum. Methods 101, 149 (1972).
[33]B. Bergersen and T. McMullen, Solid State Commun. 9, 1865 (1975).
[34]A. P. Mills, Jr. and L. N. Pfeiffer, Phys. Rev. Lett. 36, 1389 (1976).
[35]O Sueoka and S. Koide, J. Phys. Soc. Jpn. 41, 116 (1976).
[36]W. Brandt and R. Paulin, Phys. Rev. B 15, 2511 (1977).
[37]W. Brandt and M. Mourino, Bull. Am. Phys. Soc. 24, 72 (1979).
[38]R. Paulin, R. Ripon, and W. Brandt, Phys. Rev. Lett. 31, 1214 (1973).
[39]W. Swiatkowski, B. Rozenfeld, H. B. Kolodzief, and S. Szuszkiewicz, Acta Phys. Pol. A 47, 79 (1975).
[40]B. T. A. McKee, A. T. Stewart, L. Morris, and H. Sang, in *Positron Annihilation,* proceedings of the 5th International Conference, Japan, 1978, edited by R. Hasiguti and K. Fujiwara (Japanese Institute of Metals, Aoba Aramaki, Sendai 980, Japan, 1979), p. 169.
[41]S. Pendyala and J. W. McGowan, Can. J. Phys. 52, 1051 (1974).
[42]Y. Matsuoka, H. Morinaga, and M. Ohkohchi, J. Phys. C 13, 4805 (1980).
[43]A. P. Mills, Jr. and L. N. Pfeiffer, Phys. Lett. 63A, 118 (1977); 69A, 471 (1979).
[44]J. Bardeen and W. Shockley, Phys. Rev. 80, 72 (1950).
[45]C. Kittel, *Introduction to Solid State Physics,* 3rd ed. (Wiley, New York, 1966), p. 122.
[46]B. Bergersen, E. Pajanne, P. Kubica, M. J. Stott, and C. H. Hodges, Solid State Commun. 15, 1377 (1974).
[47]A. P. Mills, Jr., Appl. Phys. 23, 189 (1980).
[48]A. P. Mills, Jr., Appl. Phys. Lett. 35, 427 (1979).
[49]A. P. Mills, Jr., Appl. Phys. Lett. 37, 667 (1980).